References

1. Rabinovitch M. Molecular pathogenesis of pulmonary arterial hypertension. *J Clin Invest* 2012;122:4306–4313.
2. Rabinovitch M, Gamble WJ, Miettinen OS, Reid L. Age and sex influence on pulmonary hypertension of chronic hypoxia and on recovery. *Am J Physiol* 1981;240:H62–H72.
3. Umar S, Rabinovitch M, Eghbali M. Estrogen paradox in pulmonary hypertension: current controversies and future perspectives. *Am J Respir Crit Care Med* 2012;186:125–131.
4. White RJ. Estrogen: friend or foe in pulmonary hypertension? *Am J Respir Crit Care Med* 2016;193:1084–1086.
5. Burgoyne PS, Arnold AP. A primer on the use of mouse models for identifying direct sex chromosome effects that cause sex differences in non-gonadal tissues. *Biol Sex Differ* 2016;7:68.
6. Arnold AP, Reue K, Eghbali M, Vilain E, Chen X, Ghahramani N, *et al*. The importance of having two X chromosomes. *Philos Trans R Soc Lond B Biol Sci* 2016;371:20150113.
7. Du S, Itoh N, Askarinam S, Hill H, Arnold AP, Voskuhl RR. XY sex chromosome complement, compared with XX, in the CNS confers greater neurodegeneration during experimental autoimmune encephalomyelitis. *Proc Natl Acad Sci USA* 2014;111: 2806–2811.
8. Bellott DW, Hughes JF, Skaletsky H, Brown LG, Pyntikova T, Cho T-J, *et al*. Mammalian Y chromosomes retain widely expressed dosage-sensitive regulators. *Nature* 2014;508:494–499.
9. Soubrier F, Chung WK, Machado R, Grünig E, Aldred M, Geraci M, *et al*. Genetics and genomics of pulmonary arterial hypertension. *J Am Coll Cardiol* 2013;62(25, Suppl)D13–D21.
10. Gaidatzis D, Lerch A, Hahne F, Stadler MB. QuasR: quantification and annotation of short reads in R. *Bioinformatics* 2015;31: 1130–1132.

Histopathology of Interstitial Lung Abnormalities in the Context of Lung Nodule Resections

To the Editor:

Differentiating among the various interstitial lung diseases (ILDs) involves a summation of clinical, physiologic, radiologic, and, when available, histopathologic information (1). Although studies have demonstrated that subclinical stages of ILD (termed interstitial lung abnormalities [ILAs]) can be detected by chest computed tomography (CT) in research participants with no diagnosis of ILD (2–8), little is known about the histopathologic correlates of ILAs. We hypothesized that ILAs could represent an early and/or mild stage of idiopathic pulmonary fibrosis (IPF), and would therefore yield similar histopathologic findings. To test this hypothesis, we evaluated paired chest CT scans and histopathologic samples obtained during lung nodule resections.

Methods

We retrospectively identified a cohort of 424 patients who had undergone lung nodule resection, had a chest CT scan within 3 months before surgery, and had no history of ILD, at Brigham and Women's Hospital (BWH) between January 2001 and July 2015. ILA and ILA subtype characterizations were performed as previously described (2, 3, 6–8). In all cases, at least one section of grossly uninvolved, nonneoplastic lung was submitted for histopathologic evaluation. The slides were scored by two pulmonary pathologists blind to radiologic and clinical data. A diagnosis of usual interstitial pneumonia (UIP) or other ILDs (e.g., smoking-related ILD) was made based on published criteria (1, 9), and the slides were scored for additional histopathologic findings as noted. This study was approved by the institutional review board at BWH.

Bivariate analyses were conducted using Fisher's exact tests (for categorical variables) and two-tailed *t* tests or Wilcoxon rank-sum tests (for continuous variables) when appropriate. A multivariable logistic regression analysis was performed to identify associations between ILA and histopathologic patterns, adjusting for age, sex, and pack-years smoked based on prior work (3, 7). Analyses were conducted using SAS software (version 9.4). The reported *P* values are two-sided, and values less than 0.05 were considered statistically significant.

Results

Of the 424 patients, 26 (6%) had ILA, 257 (61%) did not have ILA, and 141 (33%) had indeterminate ILA status (baseline characteristics and histopathologic patterns stratified by ILA status are presented in Table 1). There was evidence that compared with patients without ILA (or those judged to be indeterminate for ILA), patients with ILA had increased rates of pulmonary fibrosis in general and subpleural interstitial fibrosis (Figure 1A1–A3), fibroblastic foci (Figure 1C1–C4), honeycombing/UIP (Figure 1C1–C4), and atypical adenomatous hyperplasia (AAH) (Figure 1B1–B3) in particular. After adjustment for covariates, patients with ILA were more likely to have subpleural fibrosis (odds ratio [OR], 2.1; 95% confidence interval [95% CI], 1.3–3.1; $P = 0.0009$), fibroblastic foci (OR, 4.2; 95% CI, 2.2–8.1; $P < 0.0001$), and AAH (OR, 1.7; 95% CI, 1.1–2.6; $P = 0.03$) compared with those without ILA. Similar results were obtained after an additional adjustment for a history of congestive heart failure.

Of the 26 cases of ILA, 3 (12%) were centrilobular, 17 (65%) were subpleural, and 6 (23%) were mixed. There was some evidence that associations between ILA and histopathologic findings were influenced by the imaging subtype. For example, no case of fibrosis, fibroblastic foci, or honeycombing was identified in patients with centrilobular predominant ILA. In contrast, the association between AAH and ILA appeared to be limited to centrilobular predominant ILA (OR, 3.2; 95% CI, 1.5–6.4; $P = 0.002$). There was no evidence that the distance between the lung nodule and the nearest imaging findings, or the malignant status of the nodule, affected our findings of association. Of note, three patients had subpleural ILA with no pathologic evidence of fibrosis, and all of these

Supported by NIH grants T32 HL007633 (E.R.M. and R.K.P.); National Cancer Institute R01 CA203636 (M.N.); R01 HL116473 and R01 HL122424 (G.R.W.); R01 HL130974, R01 HL129920, and P01 HL114501 (I.O.R.); and R01 HL111024, R01 HL130974, RO1 HL135142, and P01 HL114501 (G.M.H.).

Author Contributions: Study design: L.M.S., H.H., and G.M.H. Acquisition, analysis, or interpretation of the data: E.R.M., R.K.P., M.V., Y.H., T.A., M.N., G.R.W., I.O.R., L.M.S., H.H., and G.M.H. Critical revision of the manuscript for important intellectual content: E.R.M., R.K.P., M.V., Y.H., T.A., M.N., G.R.W., I.O.R., L.M.S., H.H., and G.M.H. Statistical analysis: E.R.M., R.K.P., and G.M.H. Obtained funding: G.M.H.

Originally Published in Press as DOI: 10.1164/rccm.201708-1679LE on September 21, 2017

Table 1. Characteristics and Analysis of the Lung Nodule Cohort Stratified by Interstitial Lung Abnormality Status

	No ILA (*n* = 257; 61%)	Indeterminate ILA (*n* = 141; 33%)	ILA (*n* = 26; 6%)	*P* Value*	
				All Groups	ILA vs. No ILA
Demographic parameters					
Age at resection, yr, median (IQR)	64 (57–70)	71 (64–75)	73 (63–80)	<0.001	0.002
Sex, female, *n* (%)	148 (58%)	88 (62%)	18 (69%)	0.42	0.30
Race, white, *n* (%)	238 (93%)	126 (89%)	22 (85%)	0.23	0.25
BMI, kg/m^2, median (IQR)	28 (24–31)	27 (24–30)	27 (23–31)	0.54	0.94
Never smoker, *n* (%)	50 (20%)	19 (13%)	3 (12%)	0.08	0.09
Former smoker, *n* (%)	148 (59%)	98 (70%)	21 (81%)	0.08	0.09
Current smoker, *n* (%)	55 (22%)	24 (17%)	2 (8%)	0.08	0.09
Pack-years of smoking, median (IQR)	30 (7–50)	30 (10–50)	28 (19–56)	0.75	0.57
Asbestos exposure, *n* (%)	10 (5%)	15 (13%)	1 (5%)	0.06	1.0
Spirometric parameters					
FEV_1, % of predicted, median (IQR)	89 (68–102)	86 (73–98)	92 (78–104)	0.39	0.32
FVC, % of predicted, median (IQR)	93 (76–106)	88 (77–101)	98 (89–106)	0.13	0.21
FEV_1/FVC, median (IQR)	0.77 (0.69–0.82)	0.76 (0.65–0.83)	0.77 (0.71–0.80)	0.75	0.95
Selected comorbidities					
GERD, *n* (%)	93 (37%)	45 (33%)	13 (50%)	0.24	0.21
History of congestive heart failure, *n* (%)	7 (3%)	10 (7%)	3 (12%)	0.02	0.05
History of connective tissue disease, *n* (%)	15 (6%)	9 (6%)	2 (8%)	0.79	0.67
History of radiation to thorax, *n* (%)	16 (6%)	18 (13%)	0 (0%)	0.03	0.37
History of cancer†, *n* (%)	103 (41%)	69 (49%)	15 (58%)	0.10	0.10
Cancer data					
Malignant biopsy, *n* (%)	202 (79%)	112 (79%)	23 (88%)	0.53	0.31
Stage 2 or greater NSCLC, *n* (%)	51 (20%)	33 (23%)	10 (38%)	0.23	0.08
Histopathologic features					
Fibrosis					
Any fibrosis present‡, *n* (%)	133 (52%)	74 (52%)	19 (73%)	0.11	0.04
Subpleural fibrosis, *n* (%)	43 (17%)	24 (17%)	12 (46%)	0.003	0.001
Peribronchiolar fibrosis, *n* (%)	62 (24%)	32 (23%)	9 (35%)	0.41	0.24
Interstitial fibrosis, *n* (%)	53 (21%)	30 (21%)	9 (35%)	0.27	0.13
Emphysematous fibrosis§, *n* (%)	39 (15%)	24 (17%)	4 (15%)	0.88	1.0
Additional histopathologic features					
Fibroblastic foci, *n* (%)	9 (4%)	4 (3%)	7 (28%)	0.0001	0.0001
Honeycombing, *n* (%)	0 (0%)	0 (0%)	2 (8%)	0.004	0.008
UIP, *n* (%)	0 (0%)	0 (0%)	2 (8%)	0.004	0.008
Respiratory bronchiolitis, *n* (%)	156 (67%)	89 (71%)	17 (71%)	0.70	0.82
Airways disease‖, *n* (%)	126 (51%)	62 (47%)	11 (48%)	0.73	0.83
Smoking-related interstitial fibrosis¶, *n* (%)	21 (8%)	8 (6%)	1 (4%)	0.66	0.70
Pulmonary arterial hypertensive changes**, *n* (%)	213 (83%)	115 (82%)	23 (92%)	0.47	0.39
Atypical adenomatous hyperplasia, *n* (%)	43 (17%)	36 (26%)	9 (35%)	0.02	0.03
Pigment-laden macrophages, *n* (%)	188 (73%)	105 (75%)	20 (80%)	0.82	0.63
Pleural disease††, *n* (%)	18 (7%)	8 (6%)	3 (13%)	0.43	0.41

Definition of abbreviations: BMI = body mass index; GERD = gastroesophageal reflux disease; ILA = interstitial lung abnormality; IQR = interquartile range; NSCLC = non–small cell lung cancer; UIP = usual interstitial pneumonia.

Baseline demographic information and results of pathologic examinations were stratified by interstitial lung abnormality status (in some cases, not all percentages will add to 100 due to rounding). Total missing data: BMI (*n* = 24), smoking status (*n* = 4), pack-years of smoking (*n* = 11), asbestos exposure (*n* = 111), spirometry (*n* = 55), GERD (*n* = 11), history of congestive heart failure (*n* = 11), history of connective tissue disease (*n* = 2), history of radiation to thorax (*n* = 2), history of cancer (*n* = 3), subpleural fibrosis (*n* = 3), peribronchiolar fibrosis (*n* = 4), interstitial fibrosis (*n* = 1), emphysematous fibrosis (*n* = 1), fibroblastic foci (*n* = 7), respiratory bronchiolitis (*n* = 25), airways disease (*n* = 12), smoking-related interstitial fibrosis (*n* = 5), pulmonary arterial hypertensive changes (*n* = 1), atypical adenomatous hyperplasia (*n* = 1), pigment-laden macrophages (*n* = 5), and pleural disease (*n* = 8).

*Comparisons were performed using Fisher's exact test for categorical variables, and the Wilcoxon rank-sum test for continuous variables.

†History of cancer other than the nodule that was resected.

‡"Any fibrosis" is defined as having one or more of the following features: subpleural fibrosis, peribronchiolar fibrosis, interstitial fibrosis, emphysematous fibrosis, honeycombing, and UIP.

§"Emphysematous fibrosis" is defined as hyalinizing interstitial fibrosis present predominantly in association with airspace destruction and enlargement.

‖"Airways disease" includes chronic bronchitis and asthma.

¶"Smoking-related interstitial fibrosis" is defined as a combination of emphysema, bland hyalinizing interstitial fibrosis, and respiratory bronchiolitis.

**"Pulmonary arterial hypertensive changes" are vessel changes characterized by concentric smooth muscle hyperplasia.

††"Pleural disease" includes pleural adhesions, fibroelastic changes, and inflammation.

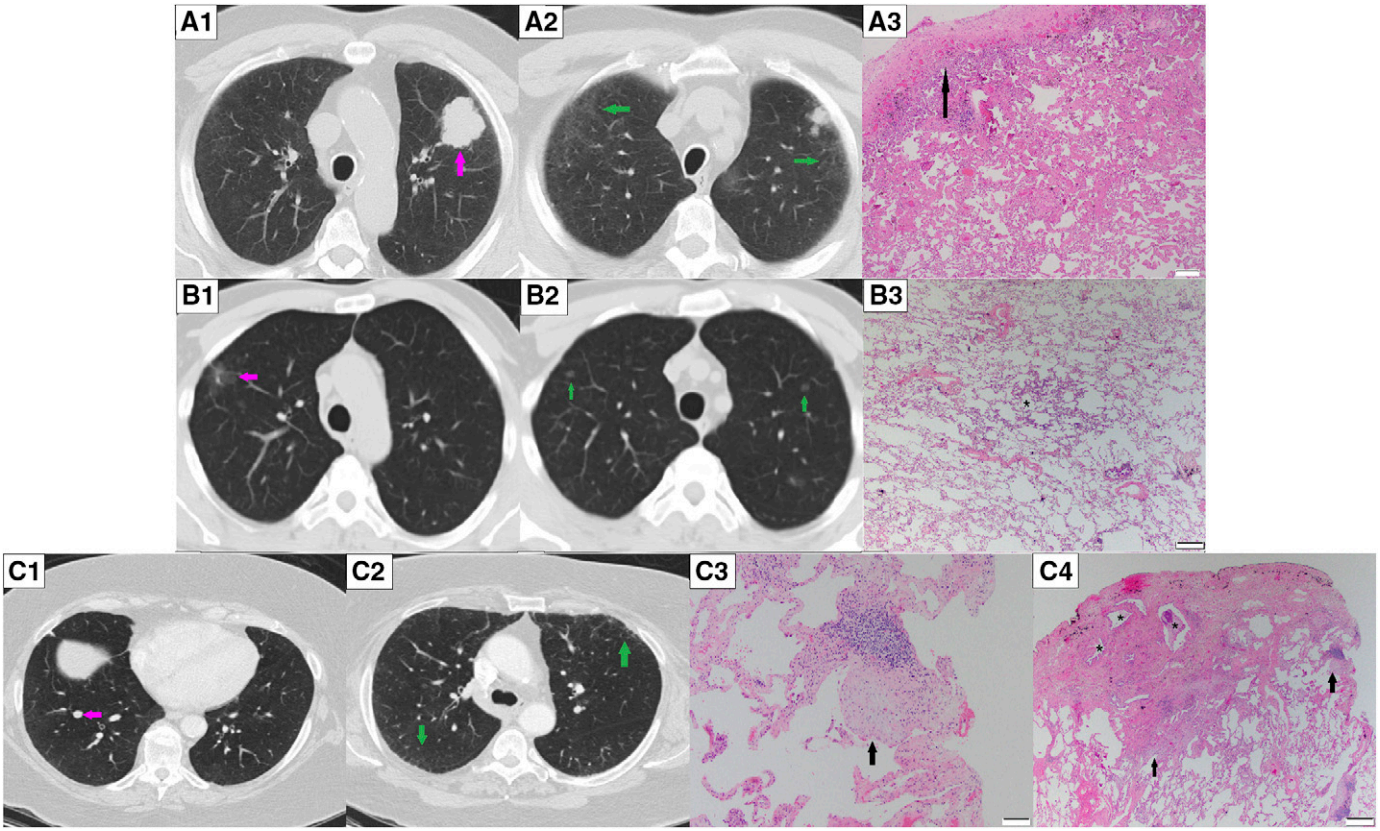

Figure 1. Individual participant examples of histopathologic patterns and associated interstitial lung abnormalities (ILAs) on computed tomography (CT). (*A1–C4*) Each lettered panel represents a different participant. *A1* shows an axial CT image with a pulmonary nodule (pink arrow). *A2* shows an axial CT image superior to the nodule demonstrating subpleural predominant ILA (green arrows). *A3* is a histologic sample demonstrating subpleural fibrosis (black arrow), hematoxylin and eosin (H&E) stain (scale bar, 2,500 μm). *B1* shows an axial CT image with a pulmonary nodule (pink arrow). *B2* is an axial CT image superior to the nodule demonstrating centrilobular predominant ILA (green arrows). *B3* is a histologic sample demonstrating atypical adenomatous hyperplasia (asterisk), H&E stain (scale bar, 500 μm). *C1* shows an axial CT image with a pulmonary nodule (pink arrow). *C2* is an axial CT image superior to the nodule demonstrating subpleural predominant ILA (green arrows). *C3* is a histologic sample demonstrating an isolated fibroblast focus (black arrow), H&E stain (scale bar, 50 μm). *C4* is a histologic view demonstrating usual interstitial pneumonia with honeycomb space (asterisks) and fibroblastic foci (black arrows), H&E stain (scale bar, 500 μm).

patients had respiratory bronchiolitis and pulmonary arterial hypertensive changes.

Finally, for five (15%) of these 26 patients (without a known clinical diagnosis of ILD), radiologic reports noted the presence of ILD and/or pulmonary fibrosis. Imaging features suggestive of ILA (e.g., subpleural fibrosis or ground-glass opacity) were noted for 20 patients (77%), whereas no interstitial features were mentioned in the reports for six (23%) patients. Twelve of the 26 patients with ILA had subpleural fibrosis and this was noted in the histopathologic reports for three patients (25%); nine had AAH and this was noted for three patients (33%); and in the reports for seven patients with fibroblastic foci and two patients with UIP/honeycombing, there was no mention of these histopathologic features.

Discussion

This study presents the first blinded, systematic comparison of chest CT imaging and histopathology for the purpose of determining pathologic features associated with ILA. These findings demonstrate that, in this BWH lung nodule cohort, subpleural fibrosis, fibroblastic foci, honeycombing/UIP, and AAH were the histopathologic features most strongly associated with ILA. In agreement with a growing body of work (2–8), this study provides evidence that ILA, in some cases, represents an early stage and/or mild form of pulmonary fibrosis.

Although histopathologic findings such as fibroblastic foci and subpleural fibrosis (which has been suggested to be a precursor to IPF) (10) are part of the criteria that help to define a UIP pattern (the histopathologic correlate of IPF), it is important to note that these features can be present in other forms of idiopathic interstitial pneumonia (1, 9). Future studies will be needed to determine whether adverse clinical outcomes are associated with these undiagnosed histopathologic findings, and whether these features commonly progress over time to more clinically apparent forms of pulmonary fibrosis.

This study has a number of limitations. First, the sample size may have limited some of our analyses, particularly those performed on subgroups. Second, because the surgical procedures were not designed to provide information about ILA, it is possible that the most informative tissue samples with respect to ILA were not

available. Third, although the pathology was examined by two experienced thoracic pathologists, the slides were reviewed by both pathologists concurrently; therefore, we cannot provide data on interobserver variability. Finally, as only limited follow-up is available, we cannot comment on the clinical outcomes associated with ILA or specific histopathologic findings within this cohort.

In conclusion, this study provides evidence that ILA—in particular, ILA with subpleural radiologic features—is most strongly associated with histopathologic findings of subpleural fibrosis as well as other histopathologic findings that are present in UIP. ■

Author disclosures are available with the text of this letter at www.atsjournals.org.

Ezra R. Miller, M.D.*
Rachel K. Putman, M.D., M.P.H.*
Marina Vivero, M.D.
Yin Hung, M.D. Ph.D.
Tetsuro Araki, M.D., Ph.D.
Mizuki Nishino, M.D., M.P.H.
George R. Washko, M.D.
Ivan O. Rosas, M.D.
Hiroto Hatabu, M.D., Ph.D.
Lynette M. Sholl, M.D.
Gary M. Hunninghake, M.D., M.P.H.
Brigham and Women's Hospital
Boston, Massachusetts

*These authors contributed equally to this article.

ORCID ID: 0000-0002-8027-7450 (R.K.P.).

References

1. Raghu G, Collard HR, Egan JJ, Martinez FJ, Behr J, Brown KK, *et al*.; ATS/ERS/JRS/ALAT Committee on Idiopathic Pulmonary Fibrosis. An official ATS/ERS/JRS/ALAT statement: idiopathic pulmonary fibrosis: evidence-based guidelines for diagnosis and management. *Am J Respir Crit Care Med* 2011;183:788–824.
2. Washko GR, Hunninghake GM, Fernandez IE, Nishino M, Okajima Y, Yamashiro T, *et al*.; COPDGene Investigators. Lung volumes and emphysema in smokers with interstitial lung abnormalities. *N Engl J Med* 2011;364:897–906.
3. Hunninghake GM, Hatabu H, Okajima Y, Gao W, Dupuis J, Latourelle JC, *et al*. MUC5B promoter polymorphism and interstitial lung abnormalities. *N Engl J Med* 2013;368:2192–2200.
4. Lederer DJ, Enright PL, Kawut SM, Hoffman EA, Hunninghake G, van Beek EJ, *et al*. Cigarette smoking is associated with subclinical parenchymal lung disease: the Multi-Ethnic Study of Atherosclerosis (MESA)-lung study. *Am J Respir Crit Care Med* 2009;180: 407–414.
5. Podolanczuk AJ, Oelsner EC, Barr RG, Hoffman EA, Armstrong HF, Austin JH, *et al*. High attenuation areas on chest computed tomography in community-dwelling adults: the MESA study. *Eur Respir J* 2016;48:1442–1452.
6. Araki T, Putman RK, Hatabu H, Gao W, Dupuis J, Latourelle JC, *et al*. Development and progression of interstitial lung abnormalities in the Framingham Heart Study. *Am J Respir Crit Care Med* 2016;194: 1514–1522.
7. Putman RK, Hatabu H, Araki T, Gudmundsson G, Gao W, Nishino M, *et al*.; Evaluation of COPD Longitudinally to Identify Predictive Surrogate Endpoints (ECLIPSE) Investigators; COPDGene Investigators. Association between interstitial lung abnormalities and all-cause mortality. *JAMA* 2016;315:672–681.
8. Doyle TJ, Washko GR, Fernandez IE, Nishino M, Okajima Y, Yamashiro T, *et al*.; COPDGene Investigators. Interstitial lung abnormalities and reduced exercise capacity. *Am J Respir Crit Care Med* 2012;185: 756–762.
9. Katzenstein AL. Smoking-related interstitial fibrosis (SRIF): pathologic findings and distinction from other chronic fibrosing lung diseases. *J Clin Pathol* 2013;66:882–887.
10. Araya J, Kawabata Y, Jinho P, Uchiyama T, Ogata H, Sugita Y. Clinically occult subpleural fibrosis and acute interstitial pneumonia a precursor to idiopathic pulmonary fibrosis? *Respirology* 2008;13: 408–412.

Household Air Pollution Is Associated with Altered Cardiac Function among Women in Kenya

To the Editor:

Exposure to household air pollution from burning biomass fuels is a major environmental risk factor contributing to the global disease burden (1). The greatest number of deaths attributable to air pollution are related to cardiovascular disease (2, 3). Household air pollution exposure is particularly dire in sub-Saharan Africa, where the majority of homes burn solid fuel indoors for both cooking and heating purposes (4). We describe the cross-sectional association between household air pollution measures of carbon monoxide (CO) and fine particulate matter (particulate matter less than or equal to 2.5 μm in aerodynamic diameter, $PM_{2.5}$) and echocardiographic characteristics of cardiac structure and function among women in western Kenya; an earlier version was presented as an oral abstract (5).

Methods

We present a cross-sectional analysis of baseline data collected between December 2013 and November 2014 from 44 women enrolled in a prospective cook stove replacement study in Turbo subdivision, a rural agricultural community in western Kenya. Houses are constructed with mud, and the kitchen is generally a poorly ventilated, separate structure. Women cook indoors using a traditional open fire cook stove using locally acquired wood as fuel. Women at least 18 years of age spending a minimum of 4 hours per day in the kitchen, residing in the community for at least 6 months, and willing to allow household air pollution assessment in their home were included in the study. Active smokers and women with chest deformities prohibiting performance of an echocardiogram were excluded. The Institutional Review Boards of Duke, Stanford, and Moi universities approved the study, and all participants provided written informed consent.

Trained study staff collected baseline demographic, medical, and physical exam data on all participants. A research echocardiographer performed transthoracic echocardiograms using a Philips CX-50 ultrasound machine (Philips Healthcare) on

This study was supported by the Duke Global Health Institute, Doris Duke International Clinical Research Scholarship, Stanford University Medical Scholars Award, and the NHLBI (contract HHSN268200900031C).

Author Contributions: All authors contributed to this manuscript. Conception and design: A.A., D.M., S.S.M., E.J.V., R.V., and G.S.B.; analysis and interpretation: A.A., K.K., M.N.E., F.A., R.V., G.A.W., and G.S.B.; and drafting and editing the manuscript: A.A., K.K., F.A., S.S.M., E.J.V., R.V., G.A.W., and G.S.B.

Originally Published in Press as DOI: 10.1164/rccm.201704-0832LE on September 19, 2017.